Available online at www.sciencedirect.com
SCIENCE DIRECT
Solid State Communications 137 (2006) 332–337
solid state communications
www.elsevier.com/locate/ssc

Electronic structure and optical absorption spectra of CdSe covered with ZnSe and ZnS epilayers

So Jeong Yun [a], Geunsik Lee [a], Jai Sam Kim [a], Seung Koo Shin [b], Young-Gui Yoon [c,*]

[a] Department of Physics, Pohang University of Science and Technology, Pohang 790-784, South Korea
[b] Department of Chemistry, Pohang University of Science and Technology, Pohang 790-784, South Korea
[c] Department of Physics, Chung-Ang University, Seoul 156-756, South Korea

Received 25 October 2005; accepted 29 October 2005 by A.H. MacDonald
Available online 21 November 2005

Abstract

Using the first-principles methods we compute the electronic structure and the absorption spectra for a wurtzite CdSe (0001) slab covered with zincblende ZnSe and ZnS epilayers. For each structure we compute the DOS and the imaginary part of the dielectric function. We find that the semiconductor passivation shifts the 'near Fermi-level' states of the bare CdSe slab down to lower energy levels. The migration suggests the decrease of surface effects and energy loss. We observe the substantial reduction of the abnormal peaks in the absorption spectra of the bare CdSe slab, which seems to be a consequence of the DOS migration. This is consistent with the experimental results that a proper passivation enhance the luminescence efficiency. We also study the case that the epilayer surface is terminated with PH_3 and find the PH_3 passivation also reduces the surface state to some extent.

PACS: 78.66.Hf; 78.68.+m; 73.20.At

Keywords: A. CdSe; A. ZnSe; A. ZnS; D. Electronic structure; D. Optical absorption

1. Introduction

Recently II–VI semiconductor quantum dots draw much attention because of their technological potential. Applications range from optoelectronic devices such as light emitting diodes [1,2], solar cells [3,4], displays [5,6], photovoltaic cells [7,8] to luminescence biological tags [9–13]. In order to understand the related phenomena and to design better materials for the relevant processes, we need to gain insights into the electronic and structural properties of these materials by the theoretical analysis. A number of the first-principles calculations have been performed to study II–VI compound semiconductors such as CdSe [14–23], ZnSe[18–30], and ZnS [16–21, 27–32].

Among them, CdSe quantum dots attract much interest because of their size-tunable emission in the visible wavelength range. The size-tunable emission results from the quantum confinement effect. The physical size of the dot set the boundary for the exciton, whose Bohr radius in bulk is much greater than the size of the dot. As a result, the exciton wavefunctions are truncated at the boundary and the surface passivation of the core material becomes an important problem. What we need to understand in designing core/shell quantum dots is how effectively electron and holes can be confined in the core while reducing the structural defects at the interface. In order to better confine electrons and holes in the core, the potential barrier and the band gap of a passivation material should be greater than those of CdSe. To this end, both ZnS and ZnSe are good candidates, although ZnS seems better for passivation than ZnSe (see Table 1 [33]). However, we should also consider the lattice mismatch between the CdSe core and the shell, which causes the defects at the interface. Smaller mismatch leads to lesser structural defects at interface. Since the lattice mismatch between CdSe and ZnSe is smaller than that between CdSe and ZnS (see Table 1), ZnSe seems better than ZnS.

Thus, we need a better understanding of electronic and structural properties of CdSe/ZnS and CdSe/ZnSe core/shell quantum dots. Surface and interfacial properties of those materials are less studied theoretically and it is desirable to use the first-principles calculations to provide a guide for designing core/shell quantum dots. However, the first-principles calculations of spherical quantum dots are very expensive, so we

* Corresponding author. Tel.: +82 2 820 5238; fax: +82 2 825 4988.
E-mail address: yyoon@cau.ac.kr (Y.-G. Yoon).

0038-1098/$ - see front matter © 2005 Elsevier Ltd. All rights reserved.
doi:10.1016/j.ssc.2005.10.029

Table 1
Band gap energy and lattice constant

	CdSe	CdS	ZnSe	ZnS
ZB band gap (eV)	1.90	2.55	2.82	3.78
WZ band gap (eV)	1.83	2.58	2.87	3.91
ZB lattice constant (Å)	6.05	5.81	5.66	5.40
WZ lattice constant: a (Å)	4.29	4.13	3.99	3.81
WZ lattice constant: c (Å)	7.01	6.74	6.62	6.52

Data are taken from Ref. [33].

reduce the dot system into the slab. We employ the pseudopotential density functional method within local density approximation (LDA) scheme to calculate structural and optical properties of CdSe covered with ZnSe and ZnS epilayers. The electronic structure and optical absorption spectra (the imaginary part of the dielectric function) are calculated.

We confirm that z-ZnSe is more stable than w-ZnSe on a wurtzite (WZ) CdSe (0001) surface. Here, z-ZnSe means cubic zincblende (ZB) ZnSe in (111) direction and w-ZnSe means hexagonal WZ ZnSe in (0001) direction. z-ZnS is defined similarly and the CdSe surface means the WZ CdSe (0001) surface throughout this paper. We compute the dielectric functions of quantum well structures CdSe/ZnSe, CdSe/ZnS, and CdSe/ZnSe/ZnS for various numbers of ZnSe and ZnS layers. Finally, we cover each surface of the epilayers with PH_3 to mimic the trioctylphosphine ligand and calculate dielectric functions to compare the passivation of PH_3 with that of semiconductors-ZnSe and ZnS. The computational methods are given in Section 2 and the results are given Section 3.

2. Method

In this study, we use the first-principles total energy calculation method. We calculate total energies, DOS's and dielectric functions of the multi-shell structures of II–VI compounds using the pseudopotential plane-wave scheme as implemented in the vienna ab-initio simulation package (VASP)[34,35]. The exchange-correlation is treated by local density approximation (LDA) parameterized by Ceperley and Alder [36]. The interaction between ions and electrons is described using the projector augmented wave (PAW) method developed by Blöchl [37,38].

In computing electronic structures of group II–VI semiconductors one is faced with the tricky problem whether cation d electrons should be treated as core states or valence states. Several recent calculations treated cation d electrons as valence electrons and showed improved descriptions of electronic structures [28,32]. We treat 4d electrons of Cd and 3d electrons of Zn as valence electrons. The cut-off energy of the planewave basis was set to 276.0 eV. In order to check the accuracy of our computation we calculate the band structures of CdSe, ZnSe, and ZnS bulk and compare with the previously computed results as reported in Refs. [14,20,28]. Our results show the narrow and little dispersion of the d band. The center of WZ CdSe d band is around -7.5 eV and its width at Γ point is about 0.8 eV. In the case of z-ZnSe and z-ZnS, the centers of d bands are around -6.6 eV and -6.5 eV, respectively. The d band width of ZnSe at Γ point is about 0.33 eV and that of ZnS is about 0.49 eV. These agree with the reported results.

Optimized lattice constants of bulk wurtzite CdSe are $a=4.24$ Å, $c=6.91$ Å, which is consistent with experimental values (see Table 1). We use these values for the lateral size of the surface, which we will consider. We use a slab model with a core of eight layers of WZ CdSe and a shell, consisting of 6L or 9L of ZnSe or 9L of ZnS or ZnSe 6L/ZnS 3L (from here on we abbreviate 'layer' by L). The thicknesses of these shells range between 19 and 28 Å. The vacuum region corresponds to 10 Å. Wurtzite CdSe has $(11\bar{2}0)$ and $(10\bar{1}0)$ cleavage surfaces in Refs. [39,40]. The lateral unit cell size of $(11\bar{2}0)$ and $(10\bar{1}0)$ is $\sqrt{8}$ and $\sqrt{\frac{8}{3}}$ times larger than that of (0001), respectively. Both cleavage surfaces are too large for computing the imaginary part of the dielectric function, which requires a fine k-grid. We chose the smallest (0001) surface to see the qualitative behavior of quantum confinement effect. Each dangling bond of the Cd atom at bottom is terminated by an H atom. We should be very careful in treating surface polarization fields due to electric polarization as illustrated in Refs. [41–43]. Several methods have been used to remove such effect. We follow a method described in Ref. [44]. A pseudo-hydrogen with charge 1.5e is used to cap Cd at the bottom side of slab.

In calculation of the total energy we used the $(11\times11\times1)$ mesh of k-points in the first Brillouin zone generated in the Monkhorst-Pack scheme [45]. Brillouin zone integration is done by the tetrahedron method with Blöchl corrections [46]. For each ion step the total energy is minimized until the change becomes less than 1.0×10^{-4} eV. All atomic positions except those of five bottom layers are relaxed by the quasi-Newton method until the energy change becomes less than 0.1×10^{-2} eV.

In computing the dielectric function, the oscillator strength was calculated as described in Ref. [47]. In order to integrate the oscillator strength, we should use a larger k-mesh. We used various number of meshes from $(31\times31\times1)$ to $(51\times51\times1)$ to test the convergence of the dielectric function. The change in energy eigenvalues is order of 1 meV. The peaks of the dielectric function are smoothed by energy broadening of 0.05 eV.

3. Results

Bulk crystals of CdSe, ZnSe, and ZnS have hexagonal WZ and cubic ZB structures. Experimentally, ZnSe epilayers grown on a WZ CdSe substrate have only the ZB structure [48,49]. We can confirm the experimental finding using the first-principles method. We study simple systems where CdSe is covered with ZnSe 6L arranged in the four ways [Fig. 1]: w-CdSe 8L/w-ZnSe 6L, w-CdSe 8L/z-ZnSe 6L, w-CdSe 8L/w-ZnSe 3L/z-ZnSe 3L, w-CdSe 8L/z-ZnSe 3L/w-ZnSe 3L. The calculated total energy of the structure with z-ZnSe 6L is about 20, 50 and 80 meV lower than that of the structure with z-ZnSe 3L/w-ZnSe 3L, w-ZnSe 3L/z-ZnSe 3L, and w-ZnSe 6L, respectively. Hence, the z-ZnSe epilayer on the WZ CdSe is more stable than the w-ZnSe epilayer, which is consistent with the results [48,49].

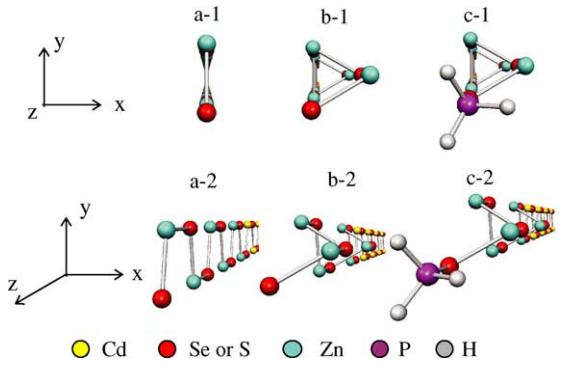

Fig. 1. Structure of slab: upper graphs are the top view and lower graphs are the side view. a-1 and a-2: the top view and the side view of w-CdSe/w-ZnSe. b-1 and b-2: the top view and the side view of w-CdSe/z-ZnSe. c-1 and c-2: the top view and the side view of w-CdSe/z-ZnSe with PH_3.

Therefore, we work with ZB epilayers of ZnSe or ZnS on a WZ CdSe slab. The symmetry of the surface is not altered by relaxation. However, relaxation leads to some degree of deviation from the bulk position. Larger deviation appears at the topmost layer and at the interface [Tables 2 and 3]. In Tables 2 and 3, the number besides the atomic symbol stands for the order of position from top to bottom. The distance between Cd and Se in the topmost layer decreases by about 3% and that of the second topmost layer increases by about 2% relative to those of the CdSe bulk. In the case of semiconductor passivation, the Se–Zn distance and the S–Zn distance in the topmost layer decreases by about 39 and 48%, respectively and that of the second topmost layer increases by about 3 and 2%, respectively. At the interface of CdSe/ZnSe and CdSe/ZnS, the distance between Cd and Se increases by about 7 and 16% and the distance between Se (or S) and Zn also increases by about 1 and 7%, respectively. In the case of CdSe/ZnS, the largest displacement occurs at the interface and the topmost layer because of larger lattice mismatch of CdSe–ZnS. When PH_3 is attached on the top Se or S atom, only PH_3 is relaxed.

In Section 3.1, we calculate the DOS and the imaginary part of the dielectric function for various structures: CdSe/z–ZnSe 6L or 9L, CdSe/z–ZnS 9L, and CdSe/z–ZnSe 6L/z–ZnS 3L. We calculate them with two thicknesses 6L and 9L. It is intended to see the effect of layer thickness on quantum confinement and the dielectric function. We suppose that the thickness of 9L is enough to see the bulk property of the passivation shell. In Section 3.2, we consider the cases that the surface is terminated by attaching PH_3 to the top Se (or S) atom after semiconductor passivation. PH_3 is used to represent a ligand and to saturate the top Se (or S).

Table 2
Deviation of the distance from top to bottom in unit (%)

	CdSe	CdSe/ ZnSe(6)	CdSe/ ZnSe(9)	CdSe/ ZnS(9)	CdSe/ZnSe/ ZnS
Se(or S)34–Zn33			−39.87	−48.15	−48.70
Zn33–Se(or S)32			3.41	2.13	2.17
Se(or S)32–Zn31			−21.72	−30.36	−31.07
Zn31–Se(or S)30			1.93	1.33	1.24
Se(or S)30–Zn29			−14.77	−21.68	−23.66
Zn29–Se(or S)28			1.56	0.90	6.63
Se(or S)28–Zn27		−39.90	−12.73	−16.48	−12.51
Zn27–Se(or S)26		3.36	1.56	1.45	1.87
Se(or S)26–Zn25		−21.96	−11.85	−15.51	−10.54
Zn25–Se(or S)24		1.83	1.60	1.82	2.04
Se(or S)24–Zn23		−15.18	−11.60	−13.51	−9.60
Zn23–Se(or S)22		1.53	1.51	2.13	1.97

Table 3
Distance from top to bottom in unit (%)(continued from Table 2)

	CdSe	CdSe/ ZnSe(6)	CdSe/ ZnSe(9)	CdSe/ ZnS(9)	CdSe/ZnSe/ ZnS
Se(or S)22–Zn21		−13.16	−12.09	−11.09	−10.06
Zn21–Se(or S)20		1.48	1.41	2.54	1.81
Se(or S)20–Zn19		−13.14	−12.64	−10.42	−10.78
Zn19–Se(or S)18		1.45	1.34	2.47	1.61
Se(or S)18–Zn17		−13.14	−12.75	−13.02	−11.60
Zn17–Se16		1.34	1.32	7.88	1.43
Se16–Cd15	−3.07	7.95	8.47	16.30	8.65
Cd15–Se14	2.08	1.71	1.71	3.67	1.78
Se14–Cd13	−3.94	8.22	8.84	17.07	8.81
Cd13–Se12	0.73	1.75	1.85	3.70	1.71
Se12–Cd11	−1.52	8.82	9.08	17.32	8.65
Cd11–Se10	0.260	1.93	1.83	3.96	1.98

3.1. Semiconductor passivation

We calculate the DOS for structures with different thicknesses of ZnSe and ZnS on a w-CdSe substrate. The DOS of bare CdSe and that of CdSe/z–ZnSe 6L/z-ZnS 3L are given in Figs. 2 and 3, respectively. The DOS is projected onto each atom, where the Fermi energy is set to 0 eV. The insets show the enlarged DOS near the Fermi-level.

In the bare CdSe, there are large DOS's around the Fermi-level, especially at Se on the surface as shown in Fig. 2(a). Moreover, there are some DOS's around the Fermi-level at Se and Cd in the bottom layer as in Fig. 2(c). These states near the Fermi level are due to the p-orbitals of Se and Cd. The DOS of the bulk CdSe is zero at the Fermi-level and has a well-defined band gap. Therefore, these states can be considered to appear due to the difference of electronic structures of bulk and slab. Since a small change of energy can lead to transitions between occupied states and empty states near the Fermi-level, these states induce the surface effects and energy loss at the surface.

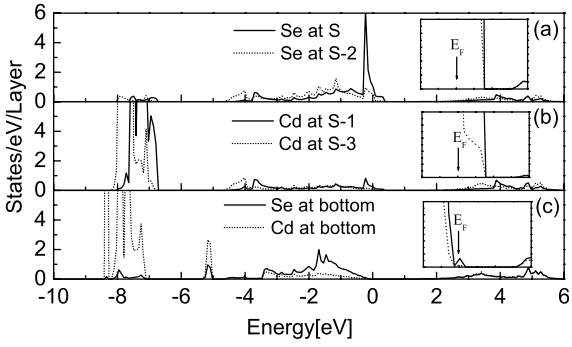

Fig. 2. DOS of bare w-CdSe. (a) solid line: the topmost Se, dotted line: the second topmost Se. (b) solid line: the topmost Cd, dotted line: the second topmost Cd. (c) solid line: the bottommost Se, dotted line: the bottommost Cd. The x-range of the inset: −0.5–1.0 (eV). The y-range of the inset: 0.0–0.025 (States/eV/Layer).

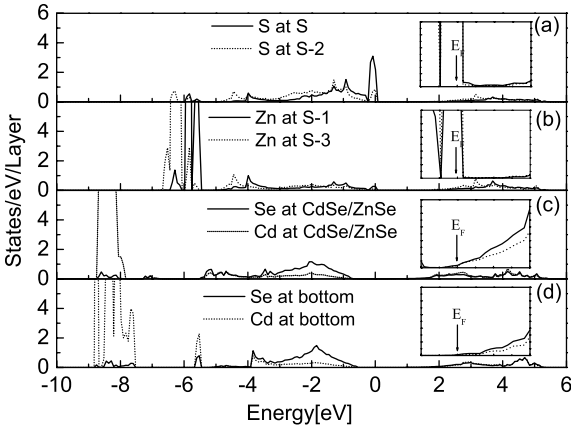

Fig. 3. DOS of w-CdSe/z-ZnSe 6L/z-ZnS 3L. (a) solid line: the topmost S, dotted line: the second topmost S. (b) solid line: the topmost Zn, dotted line: the second topmost Zn. (c) solid line: Se at the interface CdSe/ZnSe, dotted line: Cd at the interface CdSe/ZnSe. (d) solid line: the bottommost Se, dotted line: the bottommost Cd. The *x*-range of the inset: −5–1.0 (eV). The *y*-range of the inset: 0.0–0.025 (States/eV/Layer).

Passivation of the bare CdSe with the semiconductor materials, ZnSe and ZnS removes the 'near Fermi-level' states. (see Fig. 3(a) and (b)). The DOS of a passivated structure shows a trend similar to that of the bare CdSe. However, there are several different features. At the bulk position (Fig. 3(d)), the DOS of Se and Cd of the passivated structure have a similar shape but they are shifted relative to that of the bare CdSe. The DOS of the bare CdSe shows a small satellite peak near Femi-level. Such a peak disappears after passivation.

At the interface (Fig. 3(c)), the DOS of Cd and Se of a passivated structure can be compared with the DOS of Cd and Se at the surface position of the bare CdSe. After passivation, new small peaks in the DOS appear around −7 eV. This suggests the possibility that states around −7 eV after passivation are originated from states near Fermi-level before passivation. The states near Fermi-level have the p orbital character of Se and Cd. Indeed, the new states around −7 eV have the character of p-orbital of Se and s, p, d-orbital of Cd.

At the interface, the number of 'near Fermi-level' states is related to the material which faces the surface of CdSe. In CdSe/z–ZnS 9L these states increase slightly compared to CdSe/ZnSe 6L and 9L and CdSe/ZnSe/ZnS. This indicates that the degree of the lattice mismatch at the interface influences the number of 'near Fermi-level' states. In spite of the same degree of lattice mismatch, the combination CdSe/ZnSe/ZnS has less 'near Fermi-level' states at the interface than the CdSe/ZnSe system. It shows that the passivation material with less degree of lattice mismatch and a proper potential barrier effectively removes the surface states. This suggests the advantage of a multi-shell structure for enhanced optical luminescence.

We calculate the imaginary part of the dielectric function for structures as mentioned above. Fig. 4 shows the imaginary part of the dielectric function. Main plots cover the energy range of 0.0–1.0 eV and insets the range of 1.0–4.3 eV. To determine the character of peaks in the dielectric function we analyze the electric dipole transition matrix element, $\langle \mathbf{k}, c|\mathbf{P}\cdot\hat{e}|\mathbf{k}, v\rangle$. $|\mathbf{k},c\rangle$ and $|\mathbf{k},v\rangle$ stand for the wave functions of the conduction and the

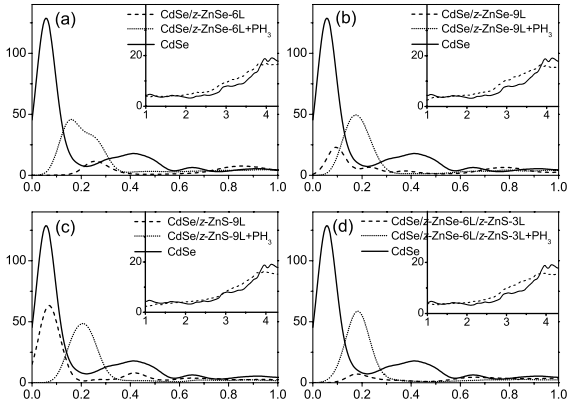

Fig. 4. Imaginary part of dielectric function. The *x*-range of the inset: 1.0–4.3 (eV). The *y*-range of the inset: 0.0–40.

valence bands respectively. **P** is the electron momentum operator and $\hat{e}$ the photon polarization vector. The valence states are scrutinized to identify which atom contributes most to peaks of the dielectric function. If the contribution of a specific atom to a valence state is over 75%, the valence state is considered to have the character of that atom. Using this method, we select the dipole matrix element corresponding to the transition from the valence state with the character of the atom to any conduction state.

In the case of bare CdSe, there is an abnormal peak around 0.0–0.1 eV and no clear absorption band edge. The first and second peaks of the dielectric function in the bare CdSe are mainly due to the top CdSe 3L. These unusually large peaks are caused by the surface states around the Fermi-level as mentioned in the DOS. These states below the band edge influence the optical efficiency of a nano-structure. Passivation with ZnSe or ZnS subdues the peaks. In Fig. 4, we see that there are still abnormal peaks around 0.0–0.3 eV after passivation. However, the amplitudes of abnormal peaks are significantly reduced compared to those of the bare CdSe. As CdSe is covered with z-ZnSe and z-ZnS layers, the amplitude of the first peak is much reduced.

Using the analysis of the dipole matrix element, we can reveal the character of a peak of the passivated structure. In CdSe/z-ZnSe 6L, the contribution from ZnSe layers is in the energy range (0.1, 0.8 eV) and the contribution from CdSe is over 0.7 eV. In CdSe/z-ZnSe 9L, the ZnSe contribution is dominant in the range (0, 0.9 eV) and the CdSe contribution comes out from 0.9 eV and increases gradually. In CdSe/z-ZnS 9L, the ZnS contribution is dominant in the range (0, 1 eV) and the CdSe contribution is over 1 eV. In the last case of CdSe/z-ZnSe 6L/z-ZnS 3L, the contribution of the top ZnS 3L is larger than those of ZnSe and CdSe in the range (0.1, 0.6 eV). Over 0.6 eV the contributions of ZnSe and CdSe appear. The contribution of CdSe to the dielectric function appears at the specific energy point as CdSe is covered with ZnSe and ZnS. The energies of CdSe electrons are confined below a specific energy. The surface states originated from CdSe are removed by the passivation. Since the abnormal first peak is related to the surface states, the reduced amplitude of the first peak suggests the decrease of the surface effects and energy loss at the surface.

The amplitude of the first peak of z-ZnSe 9L is larger than that of z-ZnSe 6L. z-ZnSe 9L has a smaller peak than z-ZnS 9L. That of CdSe/z–ZnSe 6L/z-ZnS 3L is the smallest among the cases considered here. Therefore, it seems that the degree of reduction of the first peak depends on the composition of passivation layers rather than the number of passivation layers [50,51].

3.2. PH_3 passivation

The semiconductor passivation shows the trend of improved optical luminescence by significantly reducing the number of states around the Fermi-level. However, there are still a few states around the Fermi-level because the top Se (or S) is not saturated and has a dangling bond. Experimentally, various ligands are used to saturate dangling bonds of the top Cd or Se. However, the chemical structures of ligand are too complicated to be exactly calculated from the first-principles. While oxygen atoms are attached [52] to the surface Cd for representing triotylphosphine oxide (TOPO) ligand, we use PH_3 to represent a ligand and to saturate the top Se (or S).

The DOS and dielectric functions are calculated for the cases where the surface is terminated by attaching PH_3 to the top Se (or S) atom after the semiconductor passivation. In Fig. 5, the DOS of the bottom and interface layers are similar to them, but the DOS of the top Se and Cd are different from those of the semiconductor passivation cases. There are still many states around the Fermi-level at P and the topmost Se. These states are the s, p-orbitals of P and the s-orbital of Se. At the interface and at the bottom layer, the DOS's at the Fermi-level are very small, but they are larger than those without PH_3 termination.

The states around the Fermi-level at P, Se (or S) and Zn lead to a larger first peak of the dielectric function in the cases of PH_3 passivation than that in the cases of semiconductor as shown in Fig. 4. The amplitude of the first peak of PH_3 passivation is smaller than that of bare CdSe but larger than that of CdSe/ZnSe and CdSe/ZnSe/ZnS. Therefore, it suggests that the PH_3 passivation can also reduce the surface state effects to some extent. (However, PH_3 is not good for passivating anion-terminated surface. This is evident from contour plot of electron charge density at ZnSe/ZnS interface and ZnSe–PH_3 bonding. From Fig. 6, we see that bonding to the anion-terminated surface is weak compared to bonding to the semiconductor passivated surface.) The PH_3 passivation makes the amplitudes of the first peaks increase compared to those of the semiconductor passivation without PH_3. It is compatible with the result [52] which shows that surface defects and traps can be efficiently eliminated by semiconductor shells rather than ligands.

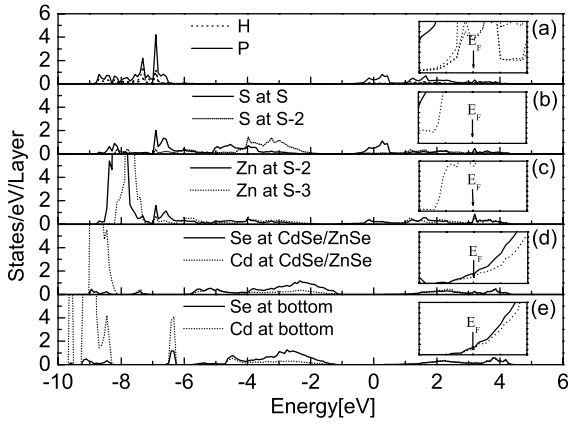

Fig. 5. DOS of w-CdSe/z-ZnSe 6L/z-ZnS 3L + PH_3. (a) solid line: the topmost P, dotted line: the topmost H. (b) solid line: the topmost S, dotted line: the second topmost S. (c) solid line: the topmost Zn, dotted line: the second topmost Zn. (d) solid line: Se at the interface CdSe/ZnSe, dotted line: Cd at the interface CdSe/ZnSe. (e) solid line: the bottommost Se, dotted line: the bottommost Cd. The *x*-range of the inset: −1.0–1.0 (eV). The *y*-range of the inset: 0.0–0.025 (States/eV/Layer).

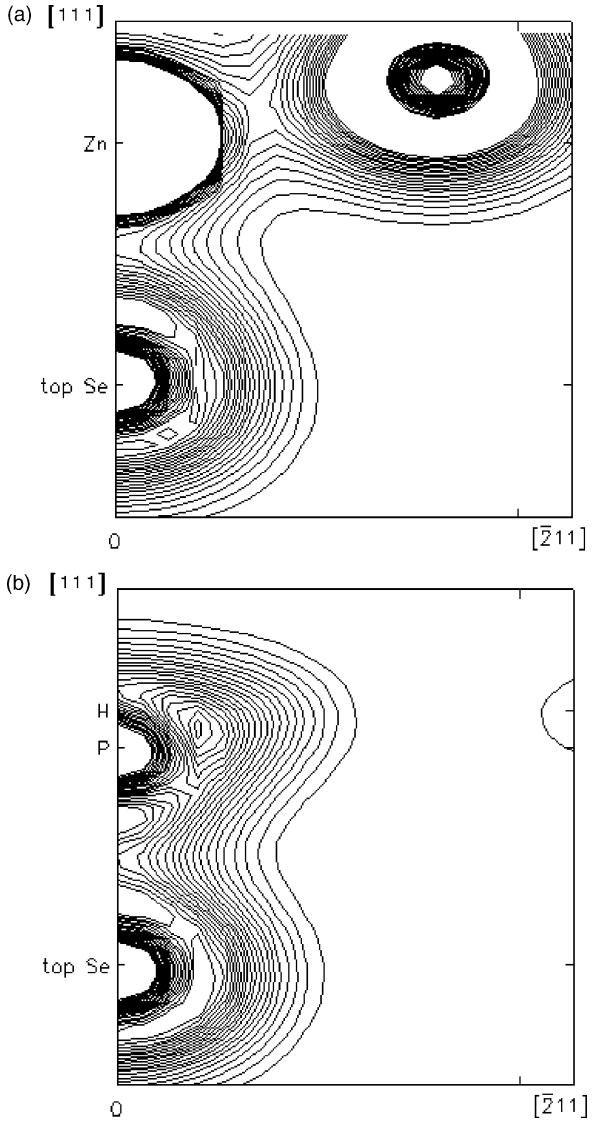

Fig. 6. The contour plots of the charge-density distribution in a [$\bar{2}$11] plane perpendicular to the (111) surface for (a) w-CdSe/z-ZnSe 6L/z-ZnS 3L and (b) w-CdSe/z-ZnSe 9L + PH_3. Indices are with respect to the cubic cell. (a) Top Se represents the Se at ZnSe/ZnS interface. (b) Top Se represents the Se at topmost layer.

4. Conclusion

To summarize, we employ the pseudopotential density functional method within local density approximation (LDA)

scheme to calculate structural and optical properties of WZ CdSe covered with ZnSe and ZnS epilayers. We determine the stable interface from the total energy. We obtain that CdSe/z–ZnSe has the lowest total energy. This is consistent with the experimental finding that ZnSe epilayers grown on a WZ CdSe substrate have only the ZB structure.

The DOS of the bare CdSe has states around the Fermi-level. The semiconductor passivation significantly removes these states around the Fermi-level and moves them to lower energies. At the interface, the DOS at the Fermi-level depends on the material, which faces the surface of CdSe. In CdSe/z–ZnS 9L these states are slightly more than CdSe/ZnSe 6L and 9L and CdSe/ZnSe/ZnS.

The imaginary part of the dielectric function of the bare CdSe has an abnormal peak below the band edge. This peak comes from the surface states as shown in the DOS. As ZnSe epilayers and ZnS epilayers are covered over bare CdSe, the intensity of the first peak in the dielectric function decreases significantly. The amplitude of the first peak of z-ZnS 9L is larger than that of z-ZnSe 9L, which is, in turn, larger than that of z-ZnSe 6L. The amplitude of the first peak of CdSe/z–ZnSe 6L/z-ZnS 3L is the smallest. The degree of reduction of the first peak is likely to depend on the composition of passivation layers rather than the number of passivation layers. Since small energy loss from surface states implies high fluorescence efficiency, our theoretical results are compatible with the experimental findings that a multi-shell semiconductor passivated structure [53–55] shows the enhanced luminescence efficiency.

The DOS of PH_3 passivation of the bottom and interface layers are similar to those of semiconductor passivation cases, but the DOS of the top Se (or S) and Zn are different from those of the semiconductor passivation cases. There are still large DOS's at P, topmost Se, and Zn. At the interface and the bottom layer, the DOS's at the Fermi-level are larger than those without PH_3 termination. The PH_3 passivation also reduces the surface state effects to some extent. However, the bonding of Se (or S) and PH_3 is weak, which makes the amplitudes of the first peaks larger than those of the semiconductor passivation without PH_3. It is compatible with the result [52] which shows that surface defects and traps can be efficiently eliminated by semiconductor shells rather than ligands.

In surface passivation of core/shell quantum dots based on CdSe, our first-principles electronic structure calculations give an insight in luminescence enhancement mechanism from explicit calculation of dielectric functions and DOS analysis. Further study of different combination of core/shell materials and larger supercells is expected to provide more concrete information of luminescence and influence of defects.

Acknowledgements

This work was supported by Postech BSRI Research Fund-2004 and the Basic Science Research Institute Special Program of Chung-Ang University in 2004 and KISTI (Korea Institute of Science and Technology Information) under 'Grand Challenge Support Program' with Dr S.M. Lee as the technical supporter. The use of the computing system of the Supercomputing Center is also greatly appreciated. SKS acknowledges the support from the R&D Program of Fusion Strategies for Advanced Technologies. This work was supported by Korean Ministry of Education through BK 21 program.

References

[1] S. Coe, et al., Nature 420 (2002) 800.
[2] N. Tessler, et al., Science 295 (2002) 1506.
[3] D. Gal, et al., Appl. Phys. Lett. 73 (1998) 3135.
[4] W.U. Huynh, et al., Science 295 (2002) 2425.
[5] V.L. Colvin, et al., Nature 370 (1994) 354.
[6] B.O. Dabbousi, et al., Appl. Phys. Lett. 66 (1995) 1316.
[7] B. O'Regan, et al., Nature 353 (1991) 737.
[8] N.C. Greenham, et al., Synth. Met. 84 (1997) 545.
[9] C.G. Van de Walle (Ed.), Wide-band-gap Semiconductors, North Holland, Amsterdam, 1993 (also published as Physica B 185, 1 (1993)).
[10] M. Bruchez, et al., Science 281 (1998) 2013.
[11] W.C.W. Chan, et al., Science 281 (1998) 2016.
[12] M.Y. Han, et al., Nat. Biotechnol. 19 (2001) 631.
[13] J.K. Jaiswal, et al., Nat. Biotechnol. 21 (2003) 47.
[14] P. Schröer, et al., Phys. Rev. B 48 (1993) 18264.
[15] O. Zakharov, et al., Phys. Rev. B 51 (1995) 4926.
[16] Y.-N. Xu, et al., Phys. Rev. B 48 (1993) 4335.
[17] D. Vogel, et al., Phys. Rev. B 52 (1995) R14316.
[18] M.-Z. Huang, et al., Phys. Rev. B 47 (1993) 9449.
[19] O. Zakharov, et al., Phys. Rev. B 50 (1994) 10780.
[20] D. Vogel, et al., Phys. Rev. B 54 (1996) 5495.
[21] S.-H. Wei, et al., Phys. Rev. B 60 (1999) 5404.
[22] M. Côté, et al., Phys. Rev. B 55 (1997) 13025.
[23] J.L.P. Hughes, et al., Phys. Rev. B 58 (1998) 7761.
[24] C.H. Park, et al., Phys. Rev. B 49 (1994) 16467.
[25] V.I. Smelyansky, et al., Phys. Rev. B 52 (1995) 4658.
[26] C.M.I. Okoye, Physica B 337 (2003) 1.
[27] C.S. Wang, et al., Phys. Rev. B 24 (1981) 3393.
[28] G.-D. Lee, et al., Phys. Rev. B 52 (1995) 1459.
[29] M. Oshikiri, et al., Phys. Rev. B 60 (1999) 10754.
[30] M. Oshikiri, et al., J. Phys. Soc. Jpn. 69 (2000) 2113.
[31] J.L. Martins, et al., Phys. Rev. B 43 (1991) 2213.
[32] P. Schröer, et al., Phys. Rev. B 47 (1993) 6971.
[33] K.-H. Hellwege, O. Madelung (Eds.), Numerical Data and Functional Relationships in Science and Technology Landolt-Börnstein, New Series, Group III vols. 17a and 22a, Springer, New York, 1982.
[34] G. Kresse, et al., Phys. Rev. B 47 (1993) R558.
[35] G. Kresse, et al., Phys. Rev. B 54 (1996) 11169.
[36] D.M. Ceperley, et al., Phys. Rev. Lett. 45 (1980) 566.
[37] P.E. Blöchl, Phys. Rev. B 50 (1994) 17953.
[38] G. Kresse, et al., Phys. Rev. B 59 (1999) 1758.
[39] B. Siemens, et al., Phys. Rev. B 56 (1997) 12321.
[40] C.B. Duke, et al., J. Vac. Sci. Technol., A 6 (1988) 692.
[41] F. Bechstedt, et al., Phys. Rev. B 62 (2000) 8003.
[42] A. Fissel, et al., Appl. Surf. Sci. 184 (2001) 37.
[43] M. Bockstedte, et al., Comput. Phys. Commun. 107 (1997) 187.
[44] K. Shiraishi, J. Phys. Soc. Jpn. 59 (1990) 3455.
[45] H.J. Monkhorst, et al., Phys. Rev. B 13 (1976) 5188.
[46] P.E. Blöchl, et al., Phys. Rev. B 49 (1994) 16223.
[47] B. Adolph, et al., Phys. Rev. B 63 (2001) 125108.
[48] N. Matsumura, et al., Jpn. J. Appl. Phys. 39 (2000) L1026.
[49] N. Matsumura, et al., J. Cryst. Growth 237-239 (2002) 1536.
[50] B.O. Dabbousi, et al., J. Phys. Chem. B 101 (1999) 9463.
[51] A.V. Baranov, et al., Phys. Rev. B 68 (2003) 165306.
[52] S. Pokrant, et al., Eur. Phys. J. D6 (1999) 255.
[53] J. Bleuse, et al., Physica E 21 (2003) 331.
[54] P. Reiss, et al., Synth. Met. 139 (2003) 649.
[55] D.V. Talapin, et al., J. Phys. Chem. B 108 (2004) 18826.